

Compactness techniques for the convergence analysis of schemes for diffusion equations

J. Droniou¹

December 3, 2024

Abstract

We give an introduction to discrete functional analysis techniques for elliptic equations. We show how these techniques are used to establish the convergence of various numerical schemes without assuming non-physical regularity on the data. For simplicity of exposure, we mostly consider linear equations, and we briefly explain how these techniques can be adapted and extended to non-linear meaningful models (Navier–Stokes equations, flows in porous media, etc.). These convergence techniques rely on discrete Sobolev norms and discrete functional analysis tools, translation to the discrete setting of functional analysis theorems.

Contents

1	Introduction	2
2	Convergence by compactness techniques	4
2.1	Model and preliminary considerations	4
2.2	General path for the convergence analysis	5
2.3	Examples	7
2.3.1	Two-point flux approximation (TPFA) finite volume scheme	7
2.3.2	Non-conforming P^1 finite element	9
3	Extension to non-linear models	12
3.1	Stationary equations	12
3.1.1	Academic example	12
3.1.2	Physical models	13
3.2	Time-dependent equations	15

<i>1 Introduction</i>	2
-----------------------	---

4 Conclusions and perspectives	16
---------------------------------------	-----------

References	17
-------------------	-----------

1 Introduction

A number of real-world problems are modelled by partial differential equations (PDEs) which involve some form of singularity. For example, oil engineers deal with underground reservoirs made of stacked geological layers with different rock properties, which translate into discontinuous data (permeability tensor, porosity, etc.) in the corresponding mathematical model. Another example from reservoir engineering is the modelling of wellbores; the relative scales of the wellbores ($\sim 10\text{-}20\text{cm}$ in diameter) and the reservoir ($\sim 1\text{-}2\text{km}$ large) justifies representing injection and production terms at the wells by Radon measures [33]. The mathematical analysis of PDEs involving singular data is challenging. The meaning of the terms in the equations has to be rethought; classical derivatives can no longer be used, and weak/distribution derivatives and Sobolev spaces must be introduced [4]. Beyond these now well-known tools, other techniques had to be developed for the most complex models to define appropriate notions of solutions, and to prove their existence (and uniqueness, if possible): renormalised solutions [10], entropy solutions [3], monotone operators and semi-groups [4], elliptic and parabolic capacity [10, 24], etc. The main purpose of this analysis is to ensure that the models are well-posed, i.e. that they make sense from a mathematical perspective. It is rarely possible to give explicit forms for, or even detailed qualitative behaviour of, the solutions to the extremely complex models involved in field applications. Precise quantitative information that can be used for decision-making can be obtained only through numerical approximation.

The role of mathematics in obtaining accurate approximate solutions to PDEs is twofold. First, algorithms have to be designed to compute these solutions. But, even based on sound reasoning, in some circumstances algorithms can fail to approximate the expected model [34, Chap. III, Sec. 3]. Benchmarking (testing the algorithms in well-documented cases) is useful to ensure the quality of numerical methods, but it cannot cover all situations that may occur in field applications. The second role of mathematics in the numerical approximation of real-world models is to provide rigorous analysis of the properties and convergence of the schemes; this analysis is not restricted to particular cases, and is essential to ensure the reliability of numerical methods for PDEs.

The usual way to prove the convergence of a scheme is to establish error

estimates; if \bar{u} is the solution to the PDE and u_h is the solution provided by the scheme (where h is, for example, the mesh size), then one will try to establish a bound of the kind

$$\|u_h - \bar{u}\|_X \leq \mathcal{C}h^\alpha \quad (1)$$

where $\|\cdot\|_X$ is an adequate norm and $\alpha > 0$. Such an inequality provides an estimate on the h that must be selected in order to achieve a pre-determined accuracy of the approximation. However, major limitations exist:

- Estimates of the kind (1) can be established only if the uniqueness of the solution \bar{u} to the PDE is known (if (1) holds, then \bar{u} is unique and, actually, the proof of (1) often mimics a proof of uniqueness of \bar{u}).
- The constant \mathcal{C} usually depends on higher derivatives of \bar{u} or the PDE data, and (1) therefore requires some regularity assumptions on the solution or data.

For many non-linear real-world models, including those from reservoir engineering [35] and the famous Navier–Stokes equations, uniqueness of the solution is not known unless strong regularity properties on the solution are assumed. These properties cannot be established in field applications. Hence convergence analysis based on error estimates is doomed to be somewhat disconnected from applications. This paper presents an introduction to techniques that have been recently developed to deal with this issue. These techniques enable the convergence analysis of numerical schemes under assumptions that are compatible with real-world data and constraints.

The presentation is organised as follows. The next section details the convergence technique on a simple linear stationary diffusion equation. After recalling some basic energy estimates on the model, we present the general path (in Section 2.2) to establish the convergence of schemes without any regularity assumptions on the data; this path relies on compactness techniques and *discrete functional analysis* tools, translations to the discrete setting of functional analysis results pertaining to functions of continuous variables. Section 2.3 shows on two particular schemes (two-point finite volume scheme, and non-conforming P^1 finite element scheme) how this path is applied in practice. In Section 3 we discuss the extension of this convergence technique to non-linear and non-stationary models, more realistic representations of physical phenomena. We briefly show that virtually no adaptation is required from the technique used in the linear setting to deal with the simplest non-linear models. We then give a brief overview of physical models whose numerical analysis has been successfully tackled using discrete

functional analysis tools. These include the Navier–Stokes equations, PDEs involved in glaciology, models of oil recovery, models of melting materials, etc. Conclusions and perspectives are given in Section 4.

2 Convergence by compactness techniques

2.1 Model and preliminary considerations

Let us consider, for our initial presentation, the linear diffusion equation

$$\begin{cases} -\operatorname{div}(A\nabla\bar{u}) = f & \text{in } \Omega, \\ \bar{u} = 0 & \text{on } \partial\Omega. \end{cases} \quad (2)$$

In the context of reservoir engineering, (2) corresponds to a steady single-phase single-component Darcy problem with no gravitational effects [11]; \bar{u} is the pressure and A is the matrix-valued permeability field. This field is usually considered piecewise constant (constant in each geological layer), and it is therefore discontinuous. Equation (2) cannot be considered under the classical sense – with div and ∇ denoting standard derivatives – and must be re-written in a weak form; this form is obtained by multiplying the equation by a test function v which vanishes on $\partial\Omega$ and by using Stoke’s formula [4]:

$$\begin{cases} \text{Find } \bar{u} \in H_0^1(\Omega) \text{ such that:} \\ \forall v \in H_0^1(\Omega), \int_{\Omega} A(x)\nabla\bar{u}(x) \cdot \nabla v(x) \, dx = \int_{\Omega} f(x)v(x) \, dx. \end{cases} \quad (3)$$

Here, $H_0^1(\Omega)$ is the Sobolev space of functions $v \in L^2(\Omega)$ (square-integrable functions, equipped with the norm $\|v\|_{L^2(\Omega)}^2 = \int_{\Omega} |v(x)|^2 \, dx$), that have a weak (distribution) gradient ∇v in $L^2(\Omega)^d$ and a zero value (trace) on $\partial\Omega$. Under the following assumptions, all terms in (3) are well-defined:

$$\Omega \text{ is a bounded open set of } \mathbb{R}^d \ (d \geq 1) \text{ and } f \in L^2(\Omega), \quad (4)$$

$$\begin{aligned} A : \Omega &\mapsto \mathcal{M}_d(\mathbb{R}) \text{ is a measurable matrix-valued mapping,} \\ \exists 0 < \underline{a} \leq \bar{a} < \infty &\text{ such that } |A(x)\xi| \leq \bar{a}|\xi| \text{ and } A(x)\xi \cdot \xi \geq \underline{a}|\xi|^2 \\ &\text{for a.e. } x \in \Omega \text{ and all } \xi \in \mathbb{R}^d \ (|\cdot| \text{ is the Euclidean norm in } \mathbb{R}^d). \end{aligned} \quad (5)$$

By taking $v = \bar{u}$ in (3) and by applying Cauchy-Schwarz’ inequality on the right-hand side, we find

$$\begin{aligned} \underline{a} \|\nabla\bar{u}\|_{L^2(\Omega)}^2 &\leq \int_{\Omega} A(x)\nabla\bar{u}(x) \cdot \nabla\bar{u}(x) \, dx = \int_{\Omega} f(x)\bar{u}(x) \, dx \\ &\leq \|f\|_{L^2(\Omega)} \|\bar{u}\|_{L^2(\Omega)}. \end{aligned} \quad (6)$$

Essential to the analysis of elliptic equations is the Poincaré's inequality:

$$\forall v \in H_0^1(\Omega), \|v\|_{L^2(\Omega)} \leq \text{diam}(\Omega) \|\nabla v\|_{L^2(\Omega)}. \quad (7)$$

Plugged into (6), this inequality leads to the following energy estimate, in which the left-hand side defines the norm in $H_0^1(\Omega)$:

$$\|\bar{u}\|_{H_0^1(\Omega)} := \|\nabla \bar{u}\|_{L^2(\Omega)} \leq \frac{\text{diam}(\Omega)}{a} \|f\|_{L^2(\Omega)}. \quad (8)$$

2.2 General path for the convergence analysis

Estimate (8) shows that $H_0^1(\Omega)$ is the natural energy space of Problem (2). This estimate is at the core of the theoretical study of (2) and its non-linear variants, partly due to the Rellich's compactness theorem [4].

Theorem 1 (Rellich's compact embedding) *If Ω is a bounded subset of \mathbb{R}^d , $d \geq 1$, and if $(v_n)_{n \in \mathbb{N}}$ is bounded in $H_0^1(\Omega)$, then $(v_n)_{n \in \mathbb{N}}$ has a subsequence that converges in $L^2(\Omega)$. Furthermore, any limit in $L^2(\Omega)$ of a subsequence of $(v_n)_{n \in \mathbb{N}}$ belongs to $H_0^1(\Omega)$.*

This theorem justifies the general path for a convergence analysis that is applicable without smoothness assumption on the data or the solution, and that can be adapted to non-linear equations. As described in [14], this path comprises three steps:

- (C1) Establish *a priori* energy estimates similar to (8) on the solutions to the scheme, in a mesh- and scheme-dependent discrete norm that mimics the H_0^1 norm,
- (C2) Prove a compactness result, discrete equivalent of Theorem 1: if $(u_h)_h$ is a sequence of discrete functions that are bounded in the norms introduced in (C1), then as the mesh size h goes to 0 there is a subsequence of $(u_h)_h$ that converges (at least in $L^2(\Omega)$) to a function $\bar{u} \in H_0^1(\Omega)$,
- (C3) Prove that if $\bar{u} \in H_0^1(\Omega)$ is the limit in $L^2(\Omega)$ as $h \rightarrow 0$ of solutions to the scheme, then \bar{u} satisfies (3).

Remark 2 The existence of a solution to the PDE does not need to be known. It is obtained as a consequence of the convergence proof.

The discrete $H_0^1(\Omega)$ norm is dictated by the scheme. It must be a norm for which (i) *a priori* estimates on the numerical solutions can be obtained,

and (ii) the compactness result in (C2) holds. There is however a norm applicable to a number of numerical methods. Let us assume that Ω is polytopal (polygonal in 2D, polyhedral in 3D, etc.), and that \mathcal{M} is a mesh of Ω made of polytopal cells. We denote by $h_{\mathcal{M}} = \max_{K \in \mathcal{M}} \text{diam}(K)$ the size of \mathcal{M} , and by $X_{\mathcal{M}}$ the space of piecewise constant functions in the cells. We identify $v \in X_{\mathcal{M}}$ with the family of its values $(v_K)_{K \in \mathcal{M}}$ in the cells. $\mathcal{E}_{\mathcal{M}}$ is the set of all faces of the mesh (edges in 2D), and $|\sigma|$ denotes the $(d-1)$ -dimensional measure of a face σ (i.e. length in 2D, area in 3D). We take one point x_K in each cell K , and we let $d_{K,\sigma} = \text{dist}(x_K, \sigma)$ (see Fig. 1). If σ is an interface between two cells K and L , we define $d_{\sigma} = d_{K,\sigma} + d_{L,\sigma}$; otherwise, $d_{\sigma} = d_{K,\sigma}$ with K the unique cell whose σ is a face.

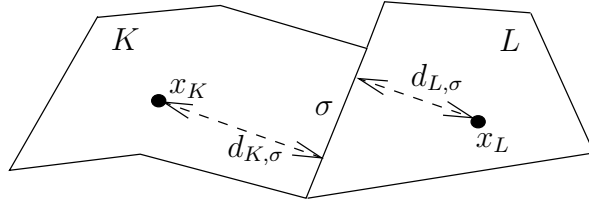


Figure 1: Notations associated with a polytopal mesh.

A discrete H_0^1 norm on $X_{\mathcal{M}}$ is defined by

$$\|v\|_{H_0^1, \mathcal{M}}^2 := \sum_{\sigma \in \mathcal{E}_{\mathcal{M}}} |\sigma| d_{\sigma} \left(\frac{v_K - v_L}{d_{\sigma}} \right)^2. \quad (9)$$

Here and in the rest of the paper, we use the convention that K and L are the cells on each side of σ , and that $v_L = 0$ if $\sigma \subset \partial\Omega$ is a face of K . This choice accounts for the homogeneous boundary conditions on $\partial\Omega$.

The major interest of this norm, in view of the path (C1)–(C3), is apparent in the two following theorems, proved in [29]. Theorem 3 is the key to reproduce at the discrete level the sequence of inequalities (6)–(8) leading to the energy estimates mentioned in (C1); this requires suitable *coercivity* properties of the scheme. Theorem 4 covers (C2). Convergence step (C3) is more scheme-dependent, and relies on *consistency* properties of the scheme. Theorems 3 and 4 are examples of discrete functional analysis results.

Theorem 3 (Discrete Poincaré’s inequality) *Let \mathcal{M} be a mesh of Ω and set*

$$\theta_{\mathcal{M}} = \max \left\{ \frac{d_{K,\sigma}}{d_{L,\sigma}} : \sigma \in \mathcal{E}_{\mathcal{M}}, K, L \text{ cells on each side of } \sigma \right\}. \quad (10)$$

If $\bar{\theta} \geq \theta_{\mathcal{M}}$ there exists C_1 only depending on $\bar{\theta}$ such that for any $v \in X_{\mathcal{M}}$ we have $\|v\|_{L^2(\Omega)} \leq C_1 \|v\|_{H_0^1, \mathcal{M}}$.

Theorem 4 (Discrete Rellich's theorem) *Let $(\mathcal{M}_n)_{n \in \mathbb{N}}$ be a sequence of discretisations of Ω such that $(\theta_{\mathcal{M}_n})_{n \in \mathbb{N}}$ is bounded and $h_{\mathcal{M}_n} \rightarrow 0$ as $n \rightarrow \infty$. If $v_n \in X_{\mathcal{M}_n}$ is such that $(\|v_n\|_{H_0^1, \mathcal{M}_n})_{n \in \mathbb{N}}$ is bounded, then $(v_n)_{n \in \mathbb{N}}$ is relatively compact in $L^2(\Omega)$. Furthermore, any limit in $L^2(\Omega)$ of a subsequence of $(v_n)_{n \in \mathbb{N}}$ belongs to $H_0^1(\Omega)$.*

2.3 Examples

Besides Theorems 3 and 4, a important feature of the discrete norm (9) is its versatility; it is adapted to numerous schemes, even with degrees of freedom that are not cell-centred. We give here a practical illustration on two methods of the usage of (C1)–(C3) and of the discrete norm (9).

2.3.1 Two-point flux approximation (TPFA) finite volume scheme

The TPFA scheme for (2) is given by flux balances (obtained by integrating (2) over the cells), and a finite difference approximation of the flux $-\int_{\sigma} A(x) \nabla \bar{u}(x) \cdot \mathbf{n}_K(x) dx$ using the two unknowns on each side of σ :

$$\forall K \in \mathcal{M} : \sum_{\sigma \in \mathcal{E}_K} F_{K,\sigma} = \int_K f(x) dx, \quad (11)$$

$$\forall K \in \mathcal{M}, \forall \sigma \in \mathcal{E}_K : F_{K,\sigma} = \tau_{\sigma}(u_K - u_L). \quad (12)$$

Here, \mathcal{E}_K is the set of faces of a cell $K \in \mathcal{M}$, and the transmissivity $\tau_{\sigma} \in (0, \infty)$ depends on A and the local mesh geometry [27]. Under usual non-degeneracy assumptions on the mesh, there exists $C_2 > 0$ only depending on \bar{a} and \underline{a} such that

$$\tau_{\sigma} \geq C_2 \frac{|\sigma|}{d_{\sigma}}. \quad (13)$$

Step (C1) The inequalities (6)–(8) that lead to the *a priori* estimates on \bar{u} are obtained by (i) multiplying (2) by $v = \bar{u}$ and integrating the resulting equation, (ii) applying Stoke's formula, and (iii) using Poincaré's inequality. Since the flux balance (11) is the discrete expression of (2), we reproduce at the discrete level this sequence of manipulations.

- (i) *Multiply and integrate:* we multiply (11) by $v_K = u_K$ and we sum on $K \in \mathcal{M}$. Accounting for (12) this gives

$$\sum_{K \in \mathcal{M}} \sum_{\sigma \in \mathcal{E}_K} \tau_{\sigma}(u_K - u_L)u_K = \sum_K \int_K f(x) dx u_K = \int_{\Omega} f(x)u(x) dx. \quad (14)$$

- (ii) *Apply Stokes formula:* this consists in gathering by faces the sum in the left-hand side of (15). The contributions of a face are $\tau_\sigma(u_K - u_L)u_K$ and $\tau_\sigma(u_L - u_K)u_L = -\tau_\sigma(u_K - u_L)u_L$. Hence, using (13) and Cauchy-Schwarz' inequality on the right-hand side, we find

$$C_2 \sum_{\sigma \in \mathcal{E}_M} \frac{|\sigma|}{d_\sigma} (u_K - u_L)^2 \leq \sum_{\sigma \in \mathcal{E}_M} \tau_\sigma (u_K - u_L)^2 \leq \|f\|_{L^2(\Omega)} \|u\|_{L^2(\Omega)}. \quad (15)$$

- (iii) *Use Poincaré's inequality:* the left-hand side of (15) is $C_2 \|u\|_{H_0^1, \mathcal{M}}^2$. Invoking the discrete Poincaré's inequality (Theorem 3), we find C_3 only depending on an upper bound of θ_M such that

$$\|u\|_{H_0^1, \mathcal{M}} \leq C_3 \|f\|_{L^2(\Omega)}. \quad (16)$$

Estimate (16) is the discrete equivalent of (8) for the solution of the TPFA scheme.

Step (C2) This step is straightforward from Estimate (16) by using the discrete Rellich theorem. This estimate shows that if $(\mathcal{M}_n)_{n \in \mathbb{N}}$ is a sequence of meshes as in Theorem 4 and if u_n is the solution of the TPFA scheme on \mathcal{M}_n , then $(\|u_n\|_{H_0^1, \mathcal{M}_n})_{n \in \mathbb{N}}$ remains bounded. Hence, up to a subsequence, u_n converges in $L^2(\Omega)$ towards some function $\bar{u} \in H_0^1(\Omega)$.

Step (C3) As mentioned above, proving that \bar{u} is the solution to (3) hinges on adequate consistency properties enjoyed by the scheme. Here, it all comes to the proper choice of transmissivities τ_σ , and to the geometry of the mesh. By taking $\varphi \in C_c^\infty(\Omega)$, multiplying (11) for $\mathcal{M} = \mathcal{M}_n$ by $\varphi(x_K)$, and summing on K we find

$$\sum_{K \in \mathcal{M}_n} \sum_{\sigma \in \mathcal{E}_K} \tau_\sigma ((u_n)_K - (u_n)_L) \varphi(x_K) = \sum_{K \in \mathcal{M}_n} \int_K f(x) \varphi(x_K) dx.$$

We then gather the sums in the left-hand side by terms involving $(u_n)_K$:

$$\sum_{K \in \mathcal{M}_n} (u_n)_K \sum_{\sigma \in \mathcal{E}_K} \tau_\sigma (\varphi(x_K) - \varphi(x_L)) = \sum_{K \in \mathcal{M}_n} \int_K f(x) \varphi(x_K) dx \quad (17)$$

where $\varphi(x_L) = 0$ if $\sigma \in \mathcal{E}_K$ lies on $\partial\Omega$. The choice of τ_σ , the geometrical assumptions put on the meshes for the TPFA method (that is, the requirement that $(x_K x_L) \perp \sigma$ for all σ face between K and L), and the smoothness

of φ ensure that $\sum_{\sigma \in \mathcal{E}_K} \tau_\sigma(\varphi(x_K) - \varphi(x_L)) = -\int_K \operatorname{div}(A\nabla\varphi) + |K|\mathcal{O}(h_{\mathcal{M}_n})$, where $|K|$ is the d -dimensional measure of K . Relation (17) thus gives

$$-\int_{\Omega} u_n(x) \operatorname{div}(A\nabla\varphi)(x) \, dx + \mathcal{O}(\|u_n\|_{L^1(\Omega)} h_{\mathcal{M}_n}) = \int_{\Omega} f(x)\varphi(x) \, dx + \mathcal{O}(h_{\mathcal{M}_n}),$$

where we used the smoothness of φ in the right-hand side. By the convergence of u_n to \bar{u} in $L^2(\Omega)$, we can pass to the limit $n \rightarrow \infty$ and we find that $\bar{u} \in H_0^1(\Omega)$ satisfies

$$\forall \varphi \in C_c^\infty(\Omega), \quad -\int_{\Omega} \bar{u}(x) \operatorname{div}(A\nabla\varphi)(x) \, dx = \int_{\Omega} f(x)\varphi(x) \, dx.$$

This is classically equivalent to (3).

Remark 5 This reasoning apparently only shows the convergence of a *subsequence* of $(u_n)_{n \in \mathbb{N}}$. However, since there is only one possible limit (namely, the unique solution \bar{u} to (3)), this actually proves that the whole sequence $(u_n)_{n \in \mathbb{N}}$ converges to \bar{u} .

2.3.2 Non-conforming P^1 finite element

Usage of the discrete norm (9) is not limited to numerical methods with only/primarily cell unknowns. Let us consider a triangulation \mathcal{T} of 2D polygonal domain Ω (what follows also generalises to tetrahedral meshes of a 3D polyhedral domain). The non-conforming Crouzeix-Raviart P^1 finite element [9] for (2) has degrees of freedom at the midpoints $(\bar{x}_\sigma)_{\sigma \in \mathcal{E}_\mathcal{T}}$ of the triangulation's edges. The discrete space $Y_\mathcal{T}$ of unknowns is made of families of reals $u = (u_\sigma)_{\sigma \in \mathcal{E}_\mathcal{T}}$, where $u_\sigma = 0$ if $\sigma \subset \partial\Omega$. These families are identified with functions $u : \Omega \rightarrow \mathbb{R}$ that are piecewise linear on the mesh, with values $(u_\sigma)_{\sigma \in \mathcal{E}_\mathcal{T}}$ at $(\bar{x}_\sigma)_{\sigma \in \mathcal{E}_\mathcal{T}}$. The non-conforming P^1 approximation of (3) is

$$\begin{cases} \text{Find } u \in Y_\mathcal{T} \text{ such that:} \\ \forall v \in Y_\mathcal{T}, \quad \int_{\Omega} A(x) \nabla_b u(x) \cdot \nabla_b v(x) \, dx = \int_{\Omega} f(x)v(x) \, dx \end{cases} \quad (18)$$

where ∇_b is the broken gradient: $(\nabla_b u)|_K$ is the constant gradient of the linear function u in the triangle $K \in \mathcal{T}$.

Step (C1) To benefit from Theorems 3 and 4, we need to introduce the norm (9), which requires some choice of cell unknowns. Here, the most

natural choice is to set u_K as the value of u at the centre of gravity \bar{x}_K of K ; since u is linear in K , this comes down to

$$\forall K \in \mathcal{T}, \quad u_K = u(\bar{x}_K) = \frac{1}{3} \sum_{\sigma \in \mathcal{E}_K} u_\sigma.$$

This choice associates (in a non-injective way) to each $u \in Y_{\mathcal{T}}$ a $\tilde{u} = (u_K)_{K \in \mathcal{T}} \in X_{\mathcal{T}}$. Two simple inequalities, both based on the fact that u is linear inside each triangle, will be useful.

Lemma 6 *Let $\eta_{\mathcal{T}}$ be the maximum over $K \in \mathcal{T}$ of the ratio of the exterior diameter of K over the interior diameter of K . Assume that $\bar{\eta} \geq \eta_{\mathcal{T}}$. Then there exists C_4 only depending on $\bar{\eta}$ such that, for all $u \in Y_{\mathcal{T}}$,*

$$\|\tilde{u}\|_{H_0^1(\mathcal{T})} \leq C_4 \|\nabla_b u\|_{L^2(\Omega)}, \quad (19)$$

$$\|\tilde{u} - u\|_{L^2(\Omega)} \leq h_{\mathcal{T}} \|\nabla_b u\|_{L^2(\Omega)}. \quad (20)$$

Proof: Let us start with (19). We notice that there exists C_5 only depending on $\bar{\eta}$ such that for all $\sigma \in \mathcal{K}$ we have $\text{dist}(\bar{x}_K, \bar{x}_\sigma) \leq C_5 d_\sigma$. Hence, since u is linear inside each triangle,

$$\begin{aligned} \frac{|\tilde{u}_K - \tilde{u}_L|}{d_\sigma} &\leq C_5 \frac{|u(\bar{x}_K) - u(\bar{x}_\sigma)|}{\text{dist}(\bar{x}_K, \bar{x}_\sigma)} + C_5 \frac{|u(\bar{x}_L) - u(\bar{x}_\sigma)|}{\text{dist}(\bar{x}_L, \bar{x}_\sigma)} \\ &\leq C_5 |(\nabla_b u)|_K + C_5 |(\nabla_b u)|_L \end{aligned} \quad (21)$$

By squaring (21), multiplying by $|\sigma|d_\sigma$, summing on the edges and using the fact that $\sum_{\sigma \in \mathcal{E}_K} |\sigma|d_\sigma \leq C_6 |K|$ with C_6 only depending on $\bar{\eta}$, we obtain (19). The proof of (20) is even simpler and follows directly from the fact that $\tilde{u}(x) - u(x) = u(\bar{x}_K) - u(x) = (\nabla_b u)|_K \cdot (\bar{x}_K - x)$ for all $x \in K$. \spadesuit

Equipped with (19) and (20), we can now delve into (C1). Plugging $v = u$ in the formulation (18) of the scheme, the coercivity of A entails

$$\underline{a} \|\nabla_b u\|_{L^2(\Omega)}^2 \leq \|f\|_{L^2(\Omega)} \|u\|_{L^2(\Omega)}.$$

Using (20) and $h_{\mathcal{T}} \leq \text{diam}(\Omega)$, this gives

$$\underline{a} \|\nabla_b u\|_{L^2(\Omega)}^2 \leq \|f\|_{L^2(\Omega)} (\|\tilde{u}\|_{L^2(\Omega)} + \text{diam}(\Omega)) \|\nabla_b u\|_{L^2(\Omega)}.$$

A bound on $\eta_{\mathcal{T}}$ implies a bound on $\theta_{\mathcal{T}}$ from (10). Hence, the discrete Poincaré's inequality (Theorem 3) and (19) lead to

$$\|\nabla_b u\|_{L^2(\Omega)} \leq \frac{C_1 C_4 + \text{diam}(\Omega)}{\underline{a}} \|f\|_{L^2(\Omega)}. \quad (22)$$

Estimate (22) is the discrete equivalent of the energy estimate (8). In conjunction with (19) it gives

$$\|\tilde{u}\|_{H_0^1, \mathcal{T}} \leq C_4 \frac{C_1 C_4 + \text{diam}(\Omega)}{\underline{a}} \|f\|_{L^2(\Omega)}. \quad (23)$$

Step (C2) Not different from the same step in the TPFA method. If $(\mathcal{T}_n)_{n \in \mathbb{N}}$ is a sequence of uniformly regular triangulations whose size tend to 0, Estimate (23) applied to $\mathcal{T} = \mathcal{T}_n$ and the discrete Rellich theorem (Theorem 4) show that $\tilde{u}_n \rightarrow \bar{u}$ in $L^2(\Omega)$ up to a subsequence, for some $\bar{u} \in H_0^1(\Omega)$. Moreover, by (20) and (22), we also have $u_n \rightarrow \bar{u}$ in $L^2(\Omega)$.

Step (C3) Let us assume for a moment that

$$\nabla_b u_n \rightarrow \nabla \bar{u} \text{ weakly in } L^2(\Omega)^d \text{ as } n \rightarrow \infty. \quad (24)$$

For $\varphi \in C_c^\infty(\Omega)$ we define the interpolant $v_n \in Y_{\mathcal{T}_n}$ by $(v_n)_\sigma = \varphi(\bar{x}_\sigma)$. The smoothness of φ ensures that $v_n \rightarrow \varphi$ in $L^\infty(\Omega)$ and $\nabla_b v_n \rightarrow \nabla \varphi$ in $L^\infty(\Omega)^d$. The convergence (24) therefore allows us to pass to the limit in (18) written for u_n and v_n . We deduce that $\bar{u} \in H_0^1(\Omega)$ satisfies $\int_\Omega A \nabla \bar{u} \cdot \nabla \varphi \, dx = \int_\Omega f \varphi \, dx$ for all smooth φ , which is equivalent to (3).

The proof of (24) relies on well-established techniques. By (22) the sequence $(\nabla_b u_n)_{n \in \mathbb{N}}$ is bounded, and therefore converges weakly in $L^2(\Omega)^d$ up to a subsequence to some χ . We just need to prove that $\chi = \nabla \bar{u}$. Take $\psi \in C_c^\infty(\Omega)^d$ and write, by Stoke's formula in each triangle,

$$\begin{aligned} \int_\Omega \nabla_b u_n(x) \cdot \psi(x) \, dx &= \sum_{K \in \mathcal{T}_n} \int_K \nabla_b u_n(x) \cdot \psi(x) \, dx \\ &= \sum_{K \in \mathcal{T}_n} \int_{\partial K} (u_n)|_K(x) \mathbf{n}_K \cdot \psi(x) \, dS(x) - \sum_{K \in \mathcal{T}_n} \int_K u_n(x) \text{div} \psi(x) \, dx \\ &= Z_n - \int_\Omega u_n(x) \text{div} \psi(x) \, dx, \end{aligned} \quad (25)$$

where \mathbf{n}_K is the outer normal to K and $(u_n)|_K$ denotes values on σ from K . Since $\psi = 0$ on $\partial\Omega$ and $\psi \cdot \mathbf{n}_K + \psi \cdot \mathbf{n}_L = 0$ on the interface σ between K and L , we have

$$\begin{aligned} \sum_{K \in \mathcal{T}_n} \sum_{\sigma \in \mathcal{E}_K} \int_\sigma (u_n)_\sigma \mathbf{n}_K \cdot \psi(x) \, dS(x) \\ = \sum_{\sigma \in \mathcal{E}, \sigma \subset \Omega} \int_\sigma (u_n)_\sigma (\mathbf{n}_K \cdot \psi(x) + \mathbf{n}_L \cdot \psi(x)) \, dS(x) = 0. \end{aligned}$$

and thus

$$Z_n = \sum_{K \in \mathcal{T}_n} \sum_{\sigma \in \mathcal{E}_K} \int_{\sigma} [(u_n)_{|K}(x) - (u_n)_{\sigma}] \mathbf{n}_K \cdot \boldsymbol{\psi}(x) \, dS(x).$$

By definition of $(u_n)_{\sigma}$ we have $\int_{\sigma} [(u_n)_{|K}(x) - (u_n)_{\sigma}] \, dS(x) = 0$. Using $|(u_n)_{|K} - (u_n)_{\sigma}| \leq \text{diam}(K) |(\nabla_b u_n)_{|K}|$ and the smoothness of $\boldsymbol{\psi}$, we infer

$$\begin{aligned} |Z_n| &= \left| \sum_{K \in \mathcal{T}_n} \sum_{\sigma \in \mathcal{E}_K} \int_{\sigma} [(u_n)_{|K}(x) - (u_n)_{\sigma}] \mathbf{n}_K \cdot [\boldsymbol{\psi}(x) - \boldsymbol{\psi}(\bar{x}_{\sigma})] \, dS(x) \right| \\ &\leq C_{\boldsymbol{\psi}} h_{\mathcal{M}_n} \sum_{K \in \mathcal{T}_n} \sum_{\sigma \in \mathcal{E}_K} |\sigma| h_K |(\nabla_b u_n)_{|K}| \leq 3C_{\boldsymbol{\psi}} C_7 h_{\mathcal{M}_n} \| |\nabla_b u_n| \|_{L^1(\Omega)} \end{aligned}$$

with C_7 not depending on n (we used the regularity assumption on \mathcal{T}_n to write $|\sigma| h_K \leq C_7 |K|$). Invoking the discrete energy estimate (22), we deduce that $Z_n \rightarrow 0$ and we can therefore pass to the limit in (25) since $u_n \rightarrow u$ in $L^2(\Omega)$ and $\nabla_b u_n \rightarrow \boldsymbol{\chi}$ weakly in $L^2(\Omega)^d$. This gives $\int_{\Omega} \boldsymbol{\chi}(x) \cdot \boldsymbol{\psi}(x) \, dx = - \int_{\Omega} \bar{u}(x) \text{div} \boldsymbol{\psi}(x) \, dx$, which proves that $\boldsymbol{\chi} = \nabla \bar{u}$ as required.

3 Extension to non-linear models

The previous technique, based on the path (C1)–(C3) and on the discrete Rellich and Poincaré's inequalities, would not be terribly useful if it only applied to the linear diffusion equation (2). Convergence of numerical methods for this equations is well-known, and best obtained through error estimates. The power of the compactness techniques presented above is that they seamlessly apply to non-linear models, including models of physical relevance such as oil recovery, Navier–Stokes equations, etc. Presenting a complete review of these techniques on such models is beyond the scope of this paper, but we can give an overview of some of the latest developments in this area.

3.1 Stationary equations

3.1.1 Academic example

Let us first show on an academic example how the previous techniques apply to a non-linear model. We consider

$$\begin{cases} -\text{div}(A(\cdot, \bar{u}) \nabla \bar{u}) = F(\bar{u}) & \text{in } \Omega, \\ \bar{u} = 0 & \text{on } \partial\Omega \end{cases} \quad (26)$$

where $F : \mathbb{R} \mapsto \mathbb{R}$ is continuous and bounded, and $A : \Omega \times \mathbb{R} \mapsto \mathcal{M}_d(\mathbb{R})$ is a Caratheodory function (measurable w.r.t. $x \in \Omega$, continuous w.r.t. $s \in \mathbb{R}$) such that for all $s \in \mathbb{R}$ the function $A(\cdot, s)$ satisfies (5) with \underline{a} and \bar{a} not depending on s . The weak form of (26) consists in writing (3) with $f(x)$ and $A(x)$ substituted by $F(\bar{u}(x))$ and $A(x, \bar{u}(x))$, respectively.

As in the case of a linear model, establishing the convergence of a numerical method for (26) by using compactness techniques consists in mimicking estimates done on the continuous equation. Here, these estimates are obtained as for the linear model; plugging $v = \bar{u}$ in the weak form of (26) and using the coercivity of A , the bound on F and Poincaré's inequality, it is easy to see that \bar{u} satisfies

$$\|\bar{u}\|_{H_0^1(\Omega)} \leq \frac{\text{diam}(\Omega)}{\underline{a}} |\Omega|^{1/2} \|F\|_{L^\infty(\mathbb{R})}.$$

Writing a numerical method for (26) from a method for the linear equation (2) is usually quite straightforward: all $f(x)$ and $A(x)$ appearing in the definition of the method (e.g. through τ_σ for the TPFA method) have to be replaced with $F(u(x))$ and $A(x, u(x))$, where u is the approximation sought through the scheme. A quick inspection of Steps (C1) in Sections 2.3.1 and 2.3.2 shows that the discrete energy estimates (16), (22) and (23) then hold with $\|f\|_{L^2(\Omega)}$ replaced with $|\Omega|^{1/2} \|F\|_{L^\infty(\mathbb{R})}$.

Step (C2) then follows from Theorem 4 exactly as in the linear case, and we find $\bar{u} \in H_0^1(\Omega)$ such that up to a subsequence $u_n \rightarrow \bar{u}$ in $L^2(\Omega)$. This ensures that $F(u_n) \rightarrow F(\bar{u})$ in $L^2(\Omega)$, and that up to a subsequence $A(\cdot, u_n) \rightarrow A(\cdot, \bar{u})$ a.e. while remaining uniformly bounded. These convergences enable us to pass to the limit in the scheme by following the exact same technique as in Steps (C3) for the linear model. This establishes that \bar{u} is a weak solution to (26).

Remark 7 The strong convergence of u_n to \bar{u} provided by Theorem 4 is not necessary in the linear case; a weak convergence in $L^2(\Omega)$ – much easier to establish – would be sufficient to prove that \bar{u} is a solution to (3). However, the strong convergence in $L^2(\Omega)$ is essential to deal with non-linear models; the weak convergence of $(u_n)_{n \in \mathbb{N}}$ would not allow us to conclude to the convergences of $F(u_n)$ or $A(\cdot, u_n)$.

3.1.2 Physical models

As mentioned in the introduction, the strength of a convergence analysis via compactness techniques is that it applies to fully non-linear models that are relevant in a number of applications.

Elliptic equations with measure data Equations of the kind (2) appear in models of oil recovery, in which f models wells. The relative scales of the reservoir and the wellbores justifies taking a Radon measure for this source term [33, 25]. The ensuing analysis is complexified. To start with, the weak formulation (3) is no longer adapted [3, 10]. Moreover, due to the singularity of the source term, the solution has very weak regularity properties, and is not unique. This prevents any proof of error estimates for numerical approximations of these models.

Compactness techniques have been applied to establish the convergence of the TPFA finite volume scheme for diffusion and (possibly non-coercive) convection–diffusion equations with measure as source terms [36, 23]. Key elements to obtaining *a priori* estimates on the solutions to these equations are the Sobolev spaces $W_0^{1,p}(\Omega)$ (equal for $p = 2$ to $H_0^1(\Omega)$), and the Sobolev embeddings. The numerical analysis of elliptic equations with measures therefore necessitates to introduce the discrete $W_0^{1,p}$ norm on $X_{\mathcal{M}}$

$$\|v\|_{W_0^{1,p},\mathcal{M}}^p := \sum_{\sigma \in \mathcal{E}_{\mathcal{M}}} |\sigma| d_{\sigma} \left(\frac{v_K - v_L}{d_{\sigma}} \right)^p,$$

to generalise the discrete Poincaré’s and Rellich’s theorems to this norm, and to establish discrete Sobolev embeddings: if $p \in (1, d)$ and $q \leq \frac{dp}{d-p}$ then

$$\|v\|_{L^q(\Omega)} \leq C \|v\|_{W_0^{1,p},\mathcal{M}}. \quad (27)$$

Remark 8 The most efficient proofs of the discrete Poincaré’s and Rellich’s theorems are actually based on the discrete Sobolev embeddings [29, 19].

Remark 9 The numerical study of diffusion equations with measures is currently limited to the TPFA scheme. No other method seems to present the proper structure that enables the mimicking of the continuous estimates [14].

Navier–Stokes equations The regularity and uniqueness in general of the solution to the Navier–Stokes equations is a famous open problem. Unless one accepts to assume these properties, convergence of numerical methods for the Navier–Stokes equations can only be rigorously established via compactness techniques. This was done in [16] for the mixed finite volume method, and in [8] for an extension of the marker-and-cell (MAC) scheme.

As in the continuous case, dealing with the non-linear term in the numerical analysis of $-\Delta \bar{u} + (\bar{u} \cdot \nabla) \bar{u} + \nabla \bar{p} = f$ requires to use some form of discrete Sobolev embeddings. The embeddings in [16, 8] are a bit more scheme-specific than (27), but this general inequality would also be sufficient for the studies in these references.

Leray–Lions and p -Laplace equations These models are non-linear generalisations of (2), that appear in models of geology [38]. The non-linearity is more severe than in (26) since it involves both \bar{u} and $\nabla\bar{u}$. The general form of these equations is $-\operatorname{div}(a(\cdot, \bar{u}, \nabla\bar{u})) = f$ (plus boundary conditions), with $a : \Omega \times \mathbb{R} \times \mathbb{R}^d \mapsto \mathbb{R}^d$ satisfying growth, monotony and coercivity assumptions. The simplest form is probably the p -Laplace equation $-\operatorname{div}(|\nabla\bar{u}|^{p-1}\nabla\bar{u}) = f$ for $p \in (1, \infty)$, which gives back the linear Laplace equation for $p = 2$.

Even with a not depending on u , uniqueness may fail for these equations [21, Remark 3.4]. This lack of uniqueness completely prevents classical error estimates for the numerical approximations of these equations. Compactness techniques have been used to study – under no uniqueness or regularity assumptions on the solution – the convergence of at least three different schemes for Leray–Lions equations: the mixed finite volume method [13], the discrete duality finite volume method [1], and a cell-centred finite volume scheme [28]. These studies make use of discrete scheme-dependent $W_0^{1,p}$ norms and related discrete Rellich and Poincaré’s inequalities. They also require an (easy) adaptation to the discrete setting of Minty’s monotony method, to deal with the non-linearity of $a(\cdot, \bar{u}, \nabla\bar{u})$ with respect to $\nabla\bar{u}$.

3.2 Time-dependent equations

Studying non-linear time-dependent models requires space–time compactness results. The usual compactness results in the context of Sobolev spaces are variants of the Aubin–Simon theorem [2, 39]. Roughly speaking, these theorems ensures the compactness in $L^1(\Omega \times (0, T))$ of a sequence of functions, provided that their gradients remain bounded in a Lebesgue space $L^p(\Omega \times (0, T))^d$, and that their time derivatives remain bounded in the dual $(L^q(0, T; W_0^{1,r}(\Omega)))'$ of a Sobolev-valued Lebesgue space. These are the natural spaces in which solutions to parabolic PDEs can be estimated.

Carrying out the numerical analysis of these equations using compactness techniques necessitates the development of discrete versions of the Aubin–Simon theorem. This has been done in a number of settings, and enabled for example the convergence analysis of schemes for

- transient Leray–Lions equations [21], including non-local dependencies of $a(x, \bar{u}, \nabla\bar{u})$ with respect to \bar{u} (as in image segmentation [32]);
- a model of miscible fluid flows in porous media from oil recovery [6, 7];
- Stefan’s model of melting material [26];
- Richards’ model and multi-phase flows in porous media [31].

Discrete Aubin–Simon theorems are not always sufficient. Some of these studies developed other compactness tools, such as a discrete Alt–Lukhaus theorem [37], or a discrete compensated compactness result [17] – to deal with degenerate parabolic PDEs that include Stefan’s and Richards’ equations.

Usual space–time compactness results only provide strong convergence in a space–time averaged norm (e.g. $L^p(\Omega \times (0, T))$ for some $p < \infty$). A technique has recently been discovered to establish a uniform-in-time convergence (i.e. in $L^\infty(0, T; L^2(\Omega))$) of numerical approximations of non-linear degenerate parabolic equations; this technique combines discrete compactness results, fine energy estimates and convexity techniques [17, 22]. Even without assuming particular regularities on the data and the solution, it is therefore possible to obtain strong convergence properties corresponding to the needs of end-users (who are usually more interested in the behaviour of the solution at the final time, than with this behaviour averaged over time).

4 Conclusions and perspectives

We presented techniques that enable the convergence analysis of numerical schemes for PDEs under assumptions that are compatible with field applications. In particular, discontinuous coefficients or fully non-linear physically relevant models can be handled. These techniques do not require the uniqueness or regularity of the solutions, and are based on discrete functional analysis tools – that is to say the translation to the discrete setting of the functional analysis used in the study of the PDEs.

These discrete tools have been adapted to a number of schemes, including the hybrid mixed mimetic family [20] (which contains the hybrid finite volumes [29], the mimetic finite differences [5], and the mixed finite volumes [15]), the discrete duality finite volumes [1], the discontinuous Galerkin methods [12], etc.

It might appear from our brief introduction that the discrete Sobolev norms and all related results (Poincaré, Rellich, etc.) require specific adaptations for each scheme or model. This is usually not the case. A framework has been recently designed, the gradient scheme framework [30, 21, 19], that enables the unified convergence analysis of many different schemes for many diffusion PDEs. The idea is to identify a set of five properties that are not related to the models, but are intrinsic to the discrete space and operators (gradient, etc.) of the numerical methods; convergence proofs of numerical approximations of many different models can be carried out based on these five properties only (sometimes even less). Generic discrete functional analysis tools exist to ensure that several well-known schemes – including

meshless methods – satisfy those properties, and therefore that the aforementioned convergence results apply to these schemes. The gradient scheme framework covers several boundary conditions, and also guided the design of new schemes [30, 18].

References

- [1] B. Andreianov, F. Boyer, and F. Hubert. Discrete duality finite volume schemes for Leray-Lions-type elliptic problems on general 2D meshes. *Numer. Methods Partial Differential Equations*, 23(1):145–195, 2007.
- [2] J.-P. Aubin. Un théorème de compacité. *C. R. Math. Acad. Sci. Paris*, 256:5042–5044, 1963.
- [3] P. Bénilan, L. Boccardo, T. Gallouët, R. Gariepy, M. Pierre, and J. L. Vázquez. An L^1 -theory of existence and uniqueness of solutions of nonlinear elliptic equations. *Ann. Scuola Norm. Sup. Pisa Cl. Sci. (4)*, 22(2):241–273, 1995.
- [4] H. Brezis. *Functional analysis, Sobolev spaces and partial differential equations*. Universitext. Springer, New York, 2011.
- [5] F. Brezzi, K. Lipnikov, and V. Simoncini. A family of mimetic finite difference methods on polygonal and polyhedral meshes. *Math. Models Methods Appl. Sci.*, 15(10):1533–1551, 2005.
- [6] C. Chainais-Hillairet and J. Droniou. Convergence analysis of a mixed finite volume scheme for an elliptic-parabolic system modeling miscible fluid flows in porous media. *SIAM J. Numer. Anal.*, 45(5):2228–2258, 2007.
- [7] C. Chainais-Hillairet, S. Krell, and A. Mouton. Convergence analysis of a DDFV scheme for a system describing miscible fluid flows in porous media. *Numer. Methods Partial Differential Equations*, 2014.
- [8] E. Chénier, R. Eymard, T. Gallouët, and R. Herbin. An extension of the MAC scheme to locally refined meshes: convergence analysis for the full tensor time-dependent Navier–Stokes equations. *Calcolo*, 52(1):69–107, 2015.
- [9] M. Crouzeix and P.-A. Raviart. Conforming and nonconforming finite element methods for solving the stationary Stokes equations. I. *Rev.*

- Française Automat. Informat. Recherche Opérationnelle Sér. Rouge*, 7(R-3):33–75, 1973.
- [10] G. Dal Maso, F. Murat, L. Orsina, and A. Prignet. Renormalized solutions of elliptic equations with general measure data. *Ann. Scuola Norm. Sup. Pisa Cl. Sci. (4)*, 28(4):741–808, 1999.
- [11] D. Di Pietro and M. Vohralik. A review of recent advances in discretization methods, a posteriori error analysis, and adaptive algorithms for numerical modeling in geosciences. 2013. To appear in *Oil & Gas Science and Technology*. DOI: 10.2516/ogst/2013158.
- [12] D. A. Di Pietro and A. Ern. *Mathematical aspects of discontinuous Galerkin methods*, volume 69 of *Mathematics & Applications (Berlin)*. Springer, Heidelberg, 2012.
- [13] J. Droniou. Finite volume schemes for fully non-linear elliptic equations in divergence form. *M2AN Math. Model. Numer. Anal.*, 40(6):1069–1100 (2007), 2006.
- [14] J. Droniou. Finite volume schemes for diffusion equations: introduction to and review of modern methods. *Math. Models Methods Appl. Sci. (M3AS)*, 24(8):1575–1619, 2014. Special issue on Recent Techniques for PDE Discretizations on Polyhedral Meshes.
- [15] J. Droniou and R. Eymard. A mixed finite volume scheme for anisotropic diffusion problems on any grid. *Numer. Math.*, 105(1):35–71, 2006.
- [16] J. Droniou and R. Eymard. Study of the mixed finite volume method for Stokes and Navier–Stokes equations. *Numer. Methods Partial Differential Equations*, 25(1):137–171, 2009.
- [17] J. Droniou and R. Eymard. Uniform-in-time convergence of numerical methods for non-linear degenerate parabolic equations. Submitted, 2014.
- [18] J. Droniou, R. Eymard, and P. Féron. Gradient schemes for Stokes problem. 2014. Submitted.
- [19] J. Droniou, R. Eymard, T. Gallouët, C. Guichard, and R. Herbin. Gradient schemes for elliptic and parabolic problems. 2015. In preparation.

- [20] J. Droniou, R. Eymard, T. Gallouët, and R. Herbin. A unified approach to mimetic finite difference, hybrid finite volume and mixed finite volume methods. *Math. Models Methods Appl. Sci.*, 20(2):265–295, 2010.
- [21] J. Droniou, R. Eymard, T. Gallouët, and R. Herbin. Gradient schemes: a generic framework for the discretisation of linear, nonlinear and nonlocal elliptic and parabolic equations. *Math. Models Methods Appl. Sci. (M3AS)*, 23(13):2395–2432, 2012.
- [22] J. Droniou, R. Eymard, and C. Guichard. Uniform-in-time convergence of numerical schemes for Richards’ and Stefan’s models. In M. Ohlberger J. Fuhrmann and C. Rohde Eds., editors, *Finite Volumes for Complex Applications VII – Methods and Theoretical Aspects*, volume 77, pages 247–254. Springer, 2014.
- [23] J. Droniou, T. Gallouët, and R. Herbin. A finite volume scheme for a noncoercive elliptic equation with measure data. *SIAM J. Numer. Anal.*, 41(6):1997–2031, 2003.
- [24] J. Droniou, A. Porretta, and A. Prignet. Parabolic capacity and soft measures for nonlinear equations. *Potential Anal.*, 19(2):99–161, 2003.
- [25] J. Droniou and K. S. Talbot. On a miscible displacement model in porous media flow with measure data. *SIAM J. Math. Anal.*, 46(5):3158–3175, 2014.
- [26] R. Eymard, P. Féron, T. Gallouët, R. Herbin, and C. Guichard. Gradient schemes for the Stefan problem. *IJFV International Journal On Finite Volumes*, 10, 2013.
- [27] R. Eymard, T. Gallouët, and R. Herbin. Finite volume methods. In P. G. Ciarlet and J.-L. Lions, editors, *Techniques of Scientific Computing, Part III*, Handbook of Numerical Analysis, VII, pages 713–1020. North-Holland, Amsterdam, 2000.
- [28] R. Eymard, T. Gallouët, and R. Herbin. Cell centred discretisation of non linear elliptic problems on general multidimensional polyhedral grids. *J. Numer. Math.*, 17(3):173–193, 2009.
- [29] R. Eymard, T. Gallouët, and R. Herbin. Discretization of heterogeneous and anisotropic diffusion problems on general nonconforming meshes SUSHI: a scheme using stabilization and hybrid interfaces. *IMA J. Numer. Anal.*, 30(4):1009–1043, 2010.

- [30] R. Eymard, C. Guichard, and R. Herbin. Small-stencil 3D schemes for diffusive flows in porous media. *ESAIM Math. Model. Numer. Anal.*, 46(2):265–290, 2012.
- [31] R. Eymard, C. Guichard, R. Herbin, and R. Masson. Gradient schemes for two-phase flow in heterogeneous porous media and Richards equation. *ZAMM Z. Angew. Math. Mech.*, 94(7-8):560–585, 2014.
- [32] R. Eymard, A. Handlovičová, R. Herbin, K. Mikula, and O. Stašová. Gradient schemes for image processing. In *Finite volumes for complex applications VI - Problems & Perspectives*, volume 4 of *Springer Proc. Math.*, pages 429–437. Springer, Heidelberg, 2011.
- [33] P. Fabrie and T. Gallouët. Modelling wells in porous media flow. *Math. Models Methods Appl. Sci.*, 10(5):673–709, 2000.
- [34] I. Faille. *Modélisation bidimensionnelle de la genèse et de la migration des hydrocarbures dans un bassin sédimentaire*. PhD thesis, Université Joseph Fourier – Grenoble 1, 1992.
- [35] X. Feng. On existence and uniqueness results for a coupled system modeling miscible displacement in porous media. *J. Math. Anal. Appl.*, 194(3):883–910, 1995.
- [36] T. Gallouët and R. Herbin. Finite volume approximation of elliptic problems with irregular data. In *Finite volumes for complex applications II*, pages 155–162. Hermes Sci. Publ., Paris, 1999.
- [37] T. Gallouët and J. C. Latché. Compactness of discrete approximate solutions to parabolic PDEs – application to a turbulence model. *Commun. Pure Appl. Anal.*, 12(6):2371–2391, 2012.
- [38] R. Glowinski and J. Rappaz. Approximation of a nonlinear elliptic problem arising in a non-newtonian fluid flow model in glaciology. *M2AN Math. Model. Numer. Anal.*, 37(1):175–186, 2003.
- [39] J. Simon. Compact sets in $L^p(0, T; B)$. *Annali Mat. Pura appl. (IV)*, CXLVI:65–96, 1987.

Author address

1. **J. Droniou**, School of Mathematical Sciences, Monash University, Clayton, VIC 3800, AUSTRALIA.
<mailto:jerome.droniou@monash.edu>